EEG Cross-Modulation During Sleep and Wake

J.W. Kantelhardt, F. Gans, A.Y. Schumann and T. Penzel

***Abstract*—Interrelated oscillatory components on many time scales are characteristic for the complex dynamics of many physiological systems. We study the oscillations in brain-wave recordings (EEG, electro-encephalo-gram) in 190 healthy subjects during sleep. In particular, we quantify the strengths of the interactions between the oscillatory components by analyzing the cross-modulation of their instantaneous amplitudes and frequencies, separating synchronous and anti-synchronous modulation. Our approach overcomes the limitation to oscillations with similar frequencies and enables us to quantify directly nonlinear effects such as positive or negative frequency modulation. By comparing the observed patterns with those for surrogate data and model data we can extract characteristic features, some of which are modulated by sleep stages.**

***Index Terms*—multivariate time series analysis, electroencephalogram, cross-modulation, instantaneous amplitudes and frequencies, sleep, sleep stages, $1/f$ noise**

I. Introduction

Complex systems often exhibit periodicities or quasi-periodicities for wide ranges of frequencies, since feedback loops and control chains can operate on quite different characteristic time scales [1], [2]. Therefore, the linear and non-linear interactions between different parts of a given complex system can be studied by time series analysis [3], [4]. If two oscillatory processes are weakly coupled, they can become phase synchronized. Transitions in the synchronization behavior have been shown to be important characteristics of coupled oscillatory model systems. In addition, many complex systems exhibit scaling laws often used to characterize the dynamics [5]. Although scaling might be a consequence of many inter-related oscillatory rhythms, such a relationship is not established. In order to understand the dynamics of a complex system one should thus identify its components and quantify their interactions [6].

In this paper, we focus on quantifying non-linear interactions between many oscillatory or quasi-oscillatory processes in the human brain as a typical example of a complex system [7], [8]. Studying data of 190 healthy subjects (age 51.3 ± 18.9a) during sleep (two nights with 7.9 ± 0.7h of data from each subject [9]) we find characteristic cross-modulation patterns that vary with the sleep stages and relate some of them with sleep physiology. In addition, we apply our amplitude and frequency cross-modulation analysis technique [6] to surrogate data and model data based on cross-correlated $1/f$ noises. We then compare the observed features with those seen in the real data. Our approach is a direct and systematic way to screen simultaneously recorded time series for linear and non-linear interactions. Specifically, we can observe how amplitude or frequency of one emergent oscillator in a specific location affects amplitude or frequency of another oscillator in a different place and/or operating at a different frequency.

During sleep the brain is in a natural state without external influences [7]. Since sleep is required for recreation, a disturbed sleep negatively affects our daily physical and mental fitness. At least ten percent of the human population in the industrialized world suffer from sleep related disorders or sleep-wake dysfunctions. Investigating human physiology during sleep is of high interest not only for identifying sleep related disorders, but also for detecting and understanding changes in sleep patterns related to other diseases such as, e. g., Alzheimer's or Parkinson's disease. The standard procedure in a hospitals' sleep laboratory includes full-night polysomnography where many sensors and electrodes are attached to the patient's body in order to measure heartbeat, respiration, muscle activity, brain waves, and eye movements. It is well known that healthy sleep consists of approximately five cycles of roughly 1-2 hours duration. Each cycle usually evolves from non-REM sleep, i. e., from light sleep stages 1 and 2 followed by the deep sleep stages 3 and 4, to REM sleep (rapid eye movement sleep) [10]. While the specific functions of the different sleep stages are still not well understood, it is believed that deep sleep is essential for physical recreation, while REM sleep is important for mental recreation.

II. Amplitude and Frequency Cross-Modulation Analysis Technique

In complex systems, oscillator frequencies are usually not fixed. They rather emerge from many interacting subcomponents (e.g., neurons) and thus exhibit time-dependent fluctuations. To quantify linear and non-linear interactions between components operating at different frequencies, we first extract instantaneous amplitudes and frequencies for each component by a Hilbert transform. Then, we study the cross-modulation of the amplitudes' and frequencies' oscillations.

As common in studying brain waves we define the components of the complex system based on (i) spatial location and (ii) frequency range (spectral output). Six oscillatory components are extracted from each raw EEG signal by FFT band-pass filtering in overlapping windows of 4096 data points, keeping only the Fourier coefficients in the desired band, see Table I. The emergent α and β wave oscillators in the visual cortex are related with active and relaxed wakefulness. Sleep spindles characterized by activity in the σ band occur mainly during light sleep, while high amplitude δ waves are dominant

J.W.K., F.G., and A.Y.S. are with the Institute of Physics, Martin-Luther-University Halle-Wittenberg, 06099 Halle, Germany, email: jan.kantelhardt@physik.uni-halle.de

F.G. present address: Max-Planck-Institute for Biogeochemistry, Biospheric Theory and Modelling Group, 07701 Jena, Germany

A.Y.S. present address: Complexity Science Group at the Department of Physics and Astronomy, University of Calgary, Canada

T.P. is with Schlafmedizinisches Zentrum der Charité Berlin, Luisenstraße 13a, 10117 Berlin, Germany

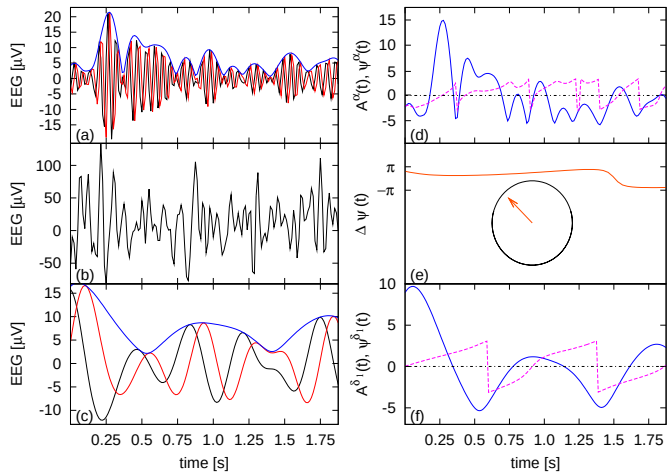

Fig. 1. Analysis of cross-modulation in EEG recordings. The raw data (b) is decomposed into x_k^α [black in (a)] and $x_k^{\delta_1}$ [in (c)], $t_k = k \cdot 0.005$s (sampling rate 200Hz). Amplitudes A_k^α and $A_k^{\delta_1}$ [Eq. (2), blue in (a,c)] are reconstructed using the Hilbert transformed signals $\tilde{x}_k^\alpha$ and $\tilde{x}_k^{\delta_1}$ [Eq. (1), red]. Next, phases ψ_k^α and $\psi_k^{\delta_1}$ [purple in (d,f)] of amplitude oscillations [blue in (d,f); shown parts differ from those in (a,c)] are calculated. Finally, complex exponentials [Eq. (3), inset in (e)] of the phase differences $\psi_k^\alpha - \psi_k^{\delta_1}$ [red in (e)] are averaged yielding μ_ν for the 30s segment.

TABLE I
FREQUENCY BANDS USED FOR EEG ANALYSIS.

band	freq. (Hz)	band	freq. (Hz)	band	freq. (Hz)
δ_1	$0.5 - 1.99$	θ	$4 - 6.99$	σ	$11.5 - 15.99$
δ_2	$2 - 3.99$	α	$7 - 11.49$	β	$16 - 22$

in deep sleep [10]. Sleep related brain waves originate from interactions between the thalamus and the cortex [7]; see [8] for a recent review on nonlinear EEG analysis.

Figures 1(a-c) show the extraction of the oscillations of α [Fig. 1(a)] and δ_1 [Fig. 1(c)] oscillator signals from a raw EEG recording [Fig. 1(b)]. Here, we consider $M = 36$ such oscillatory (or quasi-oscillatory) time series $x_k^j \equiv x^j(t_k)$, $t_k = k\Delta t$, $k = 1, \ldots, N$; $j = 1, \ldots, M$ obtained from six simultaneous EEG recordings. The electrodes were placed on the skull according to the international standard system, considering the bipolar leads O1-M2 (left back), O2-M1 (right back), C3-M2 & C4-M1 (center), and Fp1-M2 & Fp2-M1 (frontal). We employ a Hilbert transform [11] to define instantaneous amplitudes and frequencies, first complementing $x(t)$ with an imaginary part $i\tilde{x}(t)$,

$$i\tilde{x}(t) = \frac{i}{\pi}\,\text{P.V.}\int_{-\infty}^{\infty}\frac{x(t')}{t-t'}\,dt', \qquad (1)$$

where P.V. denotes Cauchy's principal value [12]. Then time series A_k and f_k can be defined by

$$A_k = \sqrt{x_k^2 + \tilde{x}_k^2},\ \varphi_k = \arctan\frac{\tilde{x}_k}{x_k},\ f_k = \frac{\varphi_k - \varphi_{k-1}}{\Delta t}, \qquad (2)$$

with the analytical signal $x_k^{(A)} = x_k + i\tilde{x}_k = A_k \exp(i\varphi_k)$.

Examples of A_k are shown in Figs. 1(a,d) for the α band and in Figs. 1(c,f) for the δ_1 band. An additional sign logic is required to obtain the full range $-\pi < \varphi_k \leq \pi$. Since φ_k is not well-defined at low A_k, very small or large f_k sometimes occur. To eliminate those artifacts, we restrict f_k to the considered band and smoothen by applying a running average filter, i. e., taking the averages over surroundings of T points, where T is the inverse of the center frequency of the band. Finally, we reduce the sampling rate to 40Hz, since A_k and f_k do not vary as fast as the original x_k.

Our goal is studying the interactions between the A_k^j and f_k^j, and this way quantifying effects like amplitude or frequency cross-modulation. We analyze the inter-relations between the 36 amplitudes A_k^j and the 36 frequencies f_k^j. For each of the $72 \times 71/2 = 2556$ pairs we calculate instantaneous phases $\psi_k^{j_1}$ and $\psi_k^{j_2}$ by applying a second Hilbert transform, Eqs. (1) and (2) with A_k^j and f_k^j instead of x_k as exemplified in Figs. 1(d,f). Then we determine the phase differences $\psi_k^{j_1} - \psi_k^{j_2}$ and average their complex exponentials over segments ν of 30s to obtain synchronization coefficients [see Fig. 1(e)]:

$$\mu_\nu = \langle \exp[i(\psi_k^{j_1} - \psi_k^{j_2})] \rangle\ . \qquad (3)$$

In the final step, we average all $|\mu_\nu|$ belonging to segments of the same physiological state (light sleep, deep sleep, REM sleep, and wake). In general the average μ will be small if the two signals oscillate or fluctuate independently, since the complex exponentials are not localized on the unit circle. In case of synchronous oscillations μ will reach values up to 1. Note that the averaging of $|\mu_\nu|$ includes $190 \times 2 \times 7.9\text{h} \times 120/\text{h} \approx 360000$ segments altogether for the EEG data analysis.

Most phase differences $\psi_k^{j_1} - \psi_k^{j_2}$ turn out to be either close to 0 (i.e., synchronous modulation) or close to $\pm\pi$ (i.e., anti-synchronous modulation). To differentiate these two cases, we separately sum the $|\mu_\nu|$ with phases of μ_ν in the interval $(-\pi/2, \pi/2)$ (synchronous modulation) and the other $|\mu_\nu|$ (anti-synchronous modulation). However, we still divide by the total number of segments in order not to over-exaggerate rare events. This way, we obtain two modulation coefficients, μ_+ and μ_-. For example, a non-zero value of μ_+ for $A_k^{\delta_1}$ and f_k^α indicates positive (synchronous) frequency modulation of the α oscillator with the amplitude of the δ_1 oscillator.

The 2556 coefficients for synchronous cross-modulation and 2556 coefficients for anti-synchronous cross-modulation are presented in color-coded matrices as follows (see Figs. 2 to 5). The modulation analysis of instantaneous amplitudes is shown in (a) while the modulation analysis of instantaneous frequencies appears in (d). In both cases, the upper triangle shows the results for synchronous modulation (μ_+), while the lower triangle shows the results for anti-synchronous modulation (μ_-). The results of amplitude-frequency cross-modulation analysis are presented in parts (b) for anti-synchronous modulation (μ_-) and (c) for synchronous modulation (μ_+). The color code shows modulation degrees increasing from blue to green, yellow and red. The six first rows and columns in each part refer to the δ_1 band of the electrodes O1-M2 (occipital left), O2-M1 (occipital right), C3-M2 (central left), C4-M1 (central right), Fp1-M2 (frontal left), and Fp2-M1 (frontal right). This is repeated for each band (see Table I). The data is rescaled in (a) to enhance details, increasing the values in the lower triangle by a factor of 8 and decreasing them in the upper triangle by 2.

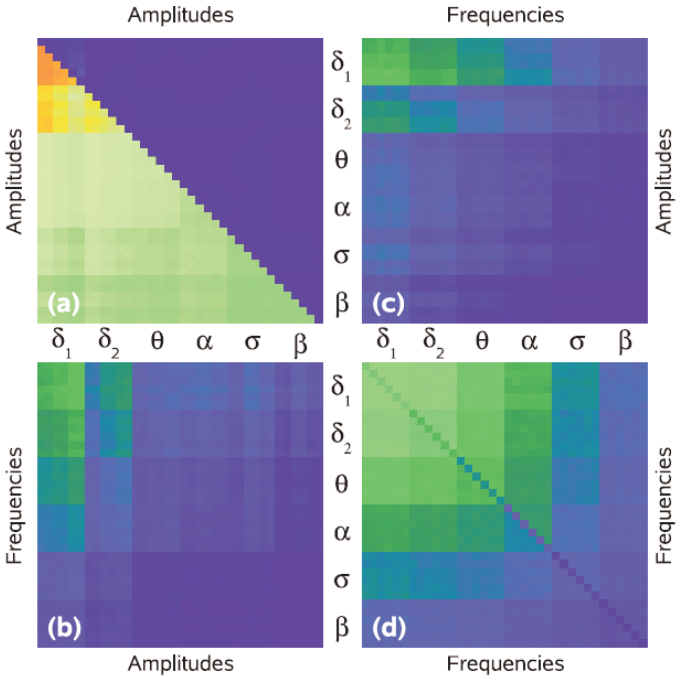

Fig. 2. Cross-modulation analysis of instantaneous amplitudes and frequencies for surrogate data consisting of pairs of signals from different nights in all 190 healthy subjects. See last paragraph of Sect. II for explanations.

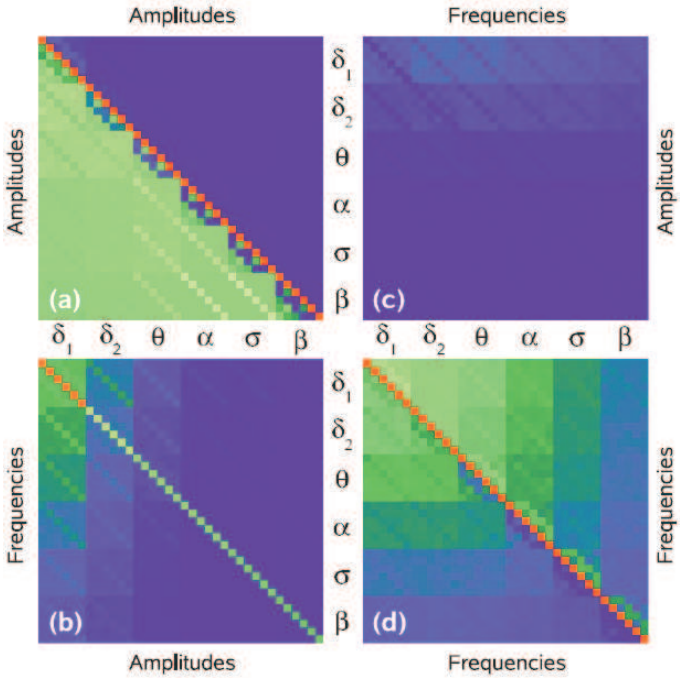

Fig. 3. Cross-modulation analysis of instantaneous amplitudes and frequencies for surrogate data consisting of artificial linearly coupled $1/f$ noises. See last paragraph of Sect. II for explanations.

III. Results for Surrogate Data and Model Data

Figure 2 shows the results of our analysis for surrogate data, where the original EEG recordings have been used, but pairs of signals recorded during different nights in the same subject were combined, e.g., δ_1 amplitude from night one and α amplitude from night two in all 190 subjects. Therefore, no cross-modulations are expected. Since nearly all pronounced colors are absent from this plot, our method does not produce artifacts due to nonstationarities in the data, measurement noise, etc. The lower left part of (a) seems to show negative amplitude-amplitude modulation; however, this is due to the up-scaling by a factor of 8. The small values of μ_- in the results from real data are nevertheless significant, since most segments actually have phase differences close to zero and contribute to μ_+ only, while the number of segments contributing to μ_- and μ_+ is identical for our surrogate data.

Figure 3 presents the results of an analysis of artificial model data with linearly coupled $1/f$ noises. For each of the 190 configurations we have generated six independent series $\xi_k^{(j)}$ ($j = 1, \ldots, 6$, $k = 1, \ldots, N$) of $1/f$ noise by Fourier filtering. Then, we have linearly coupled these series by multiplication with the following coupling matrix:

$$\begin{pmatrix} 1 & 0.1 & 0.1 & 0.05 & 0.05 & 0 \\ 0.1 & 1 & 0.05 & 0.1 & 0 & 0.05 \\ 0.1 & 0.05 & 1 & 0.1 & 0.1 & 0.05 \\ 0.05 & 0.1 & 0.1 & 1 & 0.05 & 0.1 \\ 0.05 & 0 & 0.1 & 0.05 & 1 & 0.1 \\ 0 & 0.05 & 0.05 & 0.1 & 0.1 & 1 \end{pmatrix}$$

The matrix couples signals from nearest-neighbor electrodes by 10 percent and those from second nearest neighbor electrodes by 5 percent, e.g., $\xi_k^{O1} = \xi_k^{(1)} + 0.1\xi_k^{(2)} + 0.1\xi_k^{(3)} + 0.05\xi_k^{(4)} + 0.05\xi_k^{(5)}$. No pronounced cross-modulations are seen except for the diagonal in part (b) are absent from this plot, indicating that the features to be discussed in real data indicate significant interactions. This proves that the diagonal elements in (b) are particularly representative of $1/f$ noise in complex systems.

In addition to the surrogate data tests we checked that all cross-modulation coefficients for real data remain practically the same if a second band-pass filter is employed before the second Hilbert transform to ensure narrow frequency bands and if a linear decomposition of all six EEGs by independent component analysis is performed before the analysis.

IV. Results for Real EEG Data and Discussion

Figures 4 and 5 show the results of our analysis for EEG data during wakefulness and during light sleep. As can immediately be seen, certain features as for example the diagonal in (b) indicating $1/f$ noise, are present across all sleep stages while others are only present during certain stages. A prominent feature present during nocturnal wakefulness but not during sleep stages is a positive $f^\alpha - f^\beta$ modulation [red circle in Fig. 4(d)] which is related but not identical with phase synchronization between α and β brain waves or their long-range temporal correlations during wake. The modulation of δ_1 amplitude with α frequency showing up in the top row of Fig. 5(c) is a particularly prominent feature during light sleep.

Traces of negative modulation of α amplitude with δ amplitude are observed during all sleep stages and wakefulness; they are enhanced during wake [see Fig. 4(a)] and light sleep [see Fig. 5(a)], but especially strong during deep sleep (not shown) and lowest during REM sleep (also not shown). Prevalent α waves are the typical pattern of the wake state with closed

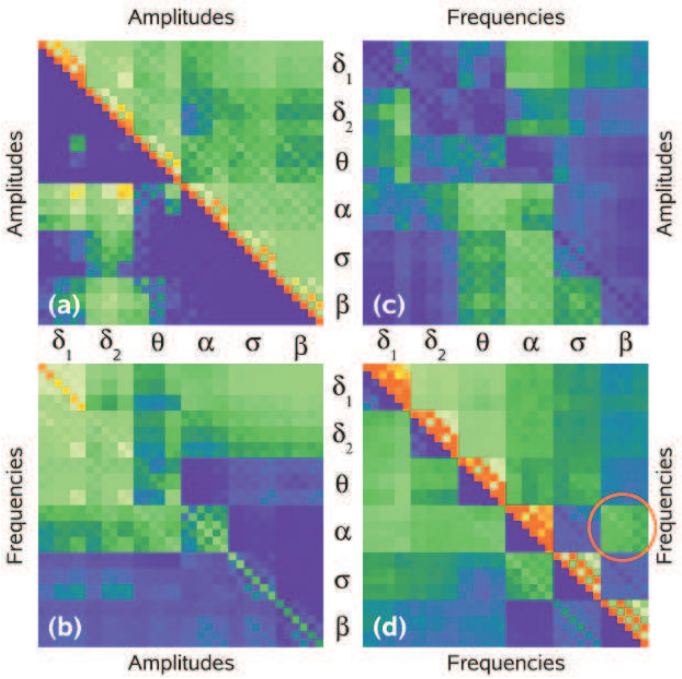

Fig. 4. Cross-modulation analysis of instantaneous amplitudes and frequencies for real EEG data during wakefulness. See text for explanations.

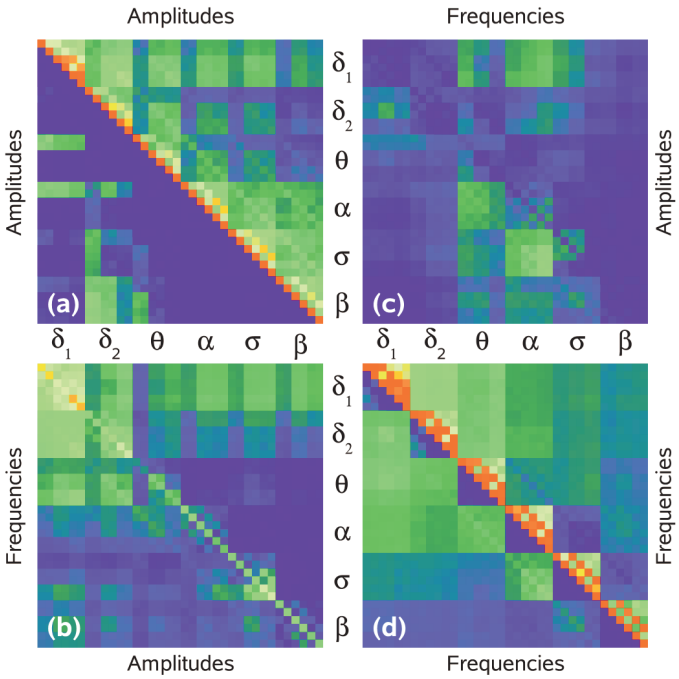

Fig. 5. Cross-modulation analysis of instantaneous amplitudes and frequencies for real EEG data during light sleep. See text for explanations.

eyes while δ waves are the main property of deep sleep. Consequently, sleep onset intrinsically results in a reduction in α activity and an increase in δ amplitude that evolves via the light sleep stage towards deep sleep. REM sleep, on the other hand, is characterized by an overall reduced EEG amplitude, high varying frequencies, and an apparent mostly 'random' and 'chaotic' appearance compared with all other stages. This explains its fainted $A^\alpha - A^\delta$ anti-modulation.

A strong negative (anti-synchronous) modulation of σ amplitudes with σ frequency is observed during light and deep sleep [see Fig. 5(b)], which appears mainly in central and frontal EEG leads. Besides such $A^\sigma - f^\sigma$ anti-modulation one observes additional positive $f^\alpha - A^\sigma$ and negative $f^\alpha - f^\sigma$ modulations [see Figs. 5(c) and (d)], which again are predominant in central- and frontal EEG leads during light and deep sleep compared with wakefulness and REM sleep. σ waves are associated with sleep spindles which have a short duration of typically 3 seconds and are predominantly found in frontal and central EEG leads during light and deep sleep. This explains the prevailing observation of the σ-related modulations. Both $f^\alpha - A^\sigma$ modulation and $f^\alpha - f^\sigma$ anti-modulation might be explained by the closeness of the two bands.

V. Summary and Conclusion

We conclude that instantaneous amplitudes and frequencies from time series can be used to study and characterize in detail linear and nonlinear inter-relations between the corresponding oscillators with very different characteristic frequencies and hence support modeling. In particular, we have demonstrated that amplitude-amplitude and frequency-frequency modulation as well as amplitude-frequency cross-modulation characterize the complex dynamics of the human brain during different sleep stages and wakefulness. Furthermore, the approach could be helpful in finding the origin of $1/f$ scaling behavior in complex systems in biology, geoscience and financing. For an application of the approach to study effects of Parkinson's disease on brain wave cross-modulation we refer to [13].

Acknowledgment

We acknowledge financial support from the European Union projects DaphNet and SOCIONICAL as well as from Deutsche Forschungsgemeinschaft (grant KA 1676/3 and PE 628/3).

References

[1] N. Boccara, *Modeling complex systems* (Springer, 2004).
[2] S.H. Strogatz, *Sync: how order emerges from chaos in the universe, nature, and daily life* (Penguin Books, 2004).
[3] H. Kantz and T. Schreiber, *Nonlinear time series analysis* (Cambridge Univ. Press, 2004).
[4] A. Pikovsky, M. Rosenblum, and J. Kurths, *Synchronization. A universal concept in nonlinear sciences* (Cambridge Univ. Press, 2001).
[5] J. Brown and G. West, *Scaling in Biology* (Oxford University Press, 2000).
[6] F. Gans, A.Y. Schumann, J.W. Kantelhardt, T. Penzel, and I. Fietze, *Phys. Rev. Lett.*, **102**:098701, 2009.
[7] G. Buzsaki, *Rhythms of the brain* (Oxford University Press, 2006).
[8] C. J. Stam, *Clin. Neurophysiol.*, **116**: 2266, 2005.
[9] G. Klösch *et al.*, *IEEE Eng. in Med. and Biol.*, **20**:51, 2001; H. Danker-Hopfe *et al.*, *J. Sleep Res.*, **13**:63, 2004.
[10] A. Rechtschaffen and A. Kales, *A manual of standardized terminology, techniques, and scoring system for sleep stages of human subjects* (U.S. Government Printing Office, Washington, 1968).
[11] D. Gabor, *Radio Commun. Eng.*, **93**:429, 1946; B. Boashash, *Proc. IEEE*, **80**(4):520–538, 1992.
[12] In practice for homogeneously sampled signals x_k, $\tilde{x}_k$ can be calculated more easily by FFT, (i) transforming x_k into Fourier space, (ii) multiplying by $-i\,\mathrm{sgn}(\omega_k)$, and (iii) transforming back to the time domain. We used partly overlapping blocks of 4096 data points; the results are identical for other block lengths.
[13] K. Stumpf, A. Y. Schumann, M. Plotnik, F. Gans, T. Penzel, I. Fietze, J. M. Hausdorff, and J. W. Kantelhardt, *EPL*, **89**:48001, 2010.